




Radiologic Manifestations of Proteus Syndrome¹

*Carlos A. Jamis-Dow, MD • Joyce Turner, MS • Leslie G. Biesecker, MD
Peter L. Choyke, MD*

Proteus syndrome is a sporadic disorder named for its highly variable manifestations. The disease causes tissue overgrowth in a mosaic pattern and may affect tissues derived from any germinal layer. The disease process is not usually apparent at birth but develops rapidly in childhood. Common manifestations include macrodactyly, vertebral abnormalities, asymmetric limb overgrowth and length discrepancy, hyperostosis, abnormal and asymmetric fat distribution, asymmetric muscle development, connective-tissue nevi, and vascular malformations. The features of Proteus syndrome indicate that the condition may be caused by a somatic alteration in a gene, but no specific genetic mutation has yet been identified. Therefore, the diagnosis and management of the disease depend heavily on clinical evaluation and imaging. Although the manifestations of Proteus syndrome are highly variable, accurate diagnosis is possible if standard diagnostic criteria are followed and if disease features are assessed in comparison with those found in similar syndromes.

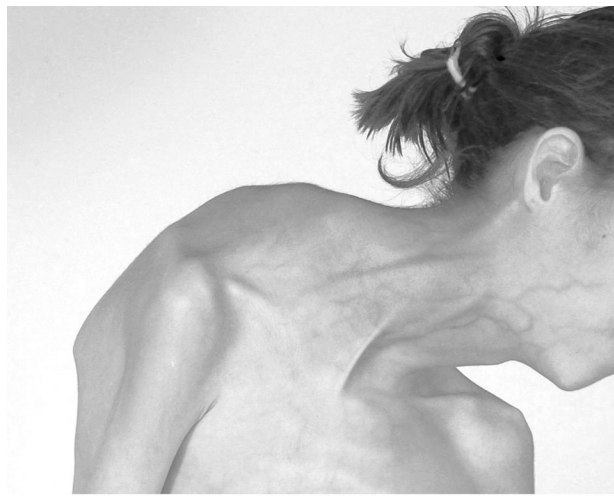
©RSNA, 2004

Index terms: Bones, abnormalities, 10.144, 40.1211, 40.1214, 40.14 • Bones, hypertrophy, 10.144, 10.916, 30.86, 40.14, 40.773, 40.862 • Extremities, abnormalities, 40.148, 46.147 • Liver, abnormalities, 761.37 • Neoplasms, diagnosis, 80.89 • Proteus syndrome • Soft tissues, neoplasms, 90.199

RadioGraphics 2004; 24:1051-1068 • Published online 10.1148/rg.244035726 • Content Codes:   

¹From the Department of Radiology, Georgetown University Hospital, Washington, DC (C.A.J.D.); Genetic Diseases Research Branch, National Human Genome Research Institute, National Institutes of Health, Bethesda, Md (J.T., L.G.B.); and Department of Radiology, Clinical Center, National Institutes of Health, Bldg 10, Room 1C-660, MSC 1182, Bethesda, MD 20892 (P.L.C.). Received October 7, 2003; revision requested November 17; revision received March 2, 2004 and accepted March 9. **Address correspondence to** P.L.C. (e-mail: pchoyke@cc.nih.gov).

©RSNA, 2004



a.

Figure 1. Neck deformity and connective-tissue nevus. Photographs of the neck (**a**) and right foot (**b**) of an 11-year-old patient show severe deformity of the chest and neck, caused by vertebral anomalies; disproportionate growth of the forefoot (the fifth toe has been amputated because of macrodactyly; see Fig 4); and plantar cerebriform connective-tissue nevus. Vertebral anomalies and connective-tissue nevi are characteristic features of Proteus syndrome.



b.

Introduction

Proteus syndrome is a rare congenital disorder that produces multifocal overgrowth of tissue. It may affect tissues derived from any of the three germinal layers (1,2). As of 1999, fewer than 200 cases of Proteus syndrome had been reported in the literature (3), and many of these cases do not meet the currently accepted diagnostic criteria (Biesecker LG, oral communication, 2003). Signs of this sporadic syndrome may include overgrowth of the long bones, asymmetric macrocephaly, striking vertebral anomalies, hyperostosis, partial gigantism of hands or feet, limb asymmetry, connective-tissue nevi, lipomas, and vascular malformations (4–6) (Fig 1). A hallmark of the disorder is the random or mosaic distribution of its manifestations throughout the body. Infants affected by the disorder usually appear normal or show only mildly asymmetric development at birth but progressively develop the characteristic features of the disease during childhood. The disease commonly progresses rapidly in childhood but may slow or stabilize during early adolescence. Premature death is not uncommon (7–9). The most common causes of premature death in Proteus syndrome are pulmonary embolism and respiratory failure (9). Predisposing fac-

tors for pulmonary embolism in these patients include vascular malformations, surgical convalescence, and, in severe cases of Proteus syndrome, very restricted mobility (9). This disorder was delineated by Cohen and Hayden in 1979 (4) and was further defined by Wiedemann (5), who proposed the term Proteus syndrome to highlight the tremendous morphologic variability of the disease entity. Because it is now accepted that Joseph Merrick (also known as the Elephant Man) was affected by Proteus syndrome, the first case report of this entity should be credited to Sir Frederick Treves (10).

The cause of Proteus syndrome is as yet unknown, but a genetic mutation that is viable only in a mosaic state has been postulated (3,11). Such a mutation could affect local production or regulation of tissue growth factor receptors (1,12). This theory would explain the sporadic nature of the syndrome, its occurrence in various ethnic groups and both sexes, and its interindividual variability, as well as the mosaic pattern of lesion distribution in all who are affected.

The unusual and highly variable manifestations of the syndrome frequently lead to misdiagnosis: Patients may have other disorders that are incorrectly diagnosed as Proteus syndrome, or may have Proteus syndrome that is incorrectly diagnosed as another disease. The Klippel-Trénaunay and hemihyperplasia–multiple lipo-

Table 1
Diagnostic Criteria for Proteus Syndrome

Category and Signs	Relative Frequency
A	
Cerebriform connective tissue nevus	Common
B	
Epidermal nevus	Common
Disproportionate overgrowth (one or more)	
Limbs	
Arms and/or legs	Common
Hands, feet, and/or digits	Common
Vertebrae	Common
Skull (calvarial thickening)	Common
External auditory meatus (hyperostosis)	Uncommon
Viscera (spleen, thymus)	Uncommon
Specific tumors before age 30 years (either one)	
Bilateral ovarian cystadenomas	Uncommon
Parotid monomorphic adenoma	Uncommon
C	
Dysregulated adipose tissue (either one)	
Lipomas	Common
Regional absence of fat	Common
Vascular malformation (one or more)	
Capillary	Common
Venous	Common
Lymphatic	Common
Abnormal facial phenotype	Uncommon
Dolichocephaly	
Minor downslanting of palpebral fissures and/or minor ptosis	
Low nasal bridge	
Wide or anteverted nares	
Open mouth when at rest	

Note.—Diagnosis is made in the presence of the general (mandatory) criteria—mosaic distribution of lesions and progressive course and sporadic occurrence—plus either the single sign from category A, two signs from category B, or three signs from category C. (Adapted, with permission, from reference 6.)

Table 2
Differential Diagnosis of Proteus Syndrome

- Klippel-Trénaunay syndrome
- Parkes Weber syndrome
- Maffucci syndrome
- Ollier disease
- Neurofibromatosis type 1
- Epidermal nevus syndrome
- Bannayan-Riley-Ruvalcaba syndrome
- Hemihyperplasia–multiple lipomatosis syndrome
- Familial lipomatosis
- Symmetric lipomatosis

Note.—Adapted, with permission, from reference 6.

Table 3
Guidelines for Patient Evaluation

- Serial clinical photography
- Initial skeletal survey with targeted follow-up radiographs
- MR imaging of all clinically affected areas or of chest and abdomen in absence of symptoms
- Dermatology consultation; biopsy when indicated
- Orthopedic consultation; surgery when indicated
- Ongoing pediatric management and testing for other genetic disorders
- Other consultations as indicated
- Referral to a family support group

Note.—Adapted, with permission, from reference 6.

matosis syndromes are the entities most commonly confused with Proteus syndrome (6). To help minimize such errors, participants in a workshop about Proteus syndrome held at the National Institutes of Health in 1998 (6) developed lists of diagnostic criteria (Table 1) and of diseases that should be considered in the differential diagnosis (Table 2), as well as guidelines for evaluation of patients (Table 3). The diagnostic tests recommended for use in patient evaluation include skeletal surveys to characterize skeletal manifestations, magnetic resonance (MR) imag-

ing of the abdomen and pelvis to exclude asymptomatic but potentially aggressive intraabdominal lipomas, MR imaging of the central nervous system to help identify abnormalities associated with neurologic symptoms, and high-spatial-resolution computed tomography (CT) of the chest to further characterize abnormal findings at prior chest radiography or pulmonary function testing. Thus, radiologists play an important role in the diagnosis, evaluation, and management of Proteus syndrome. Consistent application of the diagnostic criteria and recognition of specific signs of the disorder allow reliable clinical diagnosis. Because Proteus syndrome is rare, most radiologists are unfamiliar with its manifestations. The purpose of this article is to familiarize the reader with the radiographic manifestations of Proteus syndrome, including skeletal, soft-tissue, and visceral anomalies, as well as tumors, in a cohort of patients in whom this diagnosis was based on standardized criteria. Other syndromes and diseases that should be considered in the differential diagnosis also are surveyed.

Study Population

Using the diagnostic criteria outlined in Table 1, we identified 23 patients with Proteus syndrome. Radiologic studies were available for 21 (seven female and 14 male) patients. One hundred seventy-four studies obtained between January 15, 1989 and August 18, 2000 were reviewed. Of the 21 patients included in this review, 17 had undergone full skeletal surveys, and four had received targeted examinations of the clinically abnormal areas of their anatomy. Seventeen patients underwent CT and/or MR imaging of the head, 10 underwent CT and/or MR imaging of the chest, 17 underwent CT and/or MR imaging of the abdomen, and 15 underwent CT and/or MR imaging of the pelvis. Eight of the 14 male patients underwent scrotal ultrasonography. Table 4 gives a summary of the radiologic findings documented in this group of 21 patients during an institutional review board–approved research study at the National Human Genome Research Institute. All subjects (or, in the case of minor subjects, their parents) gave written informed consent to participate.

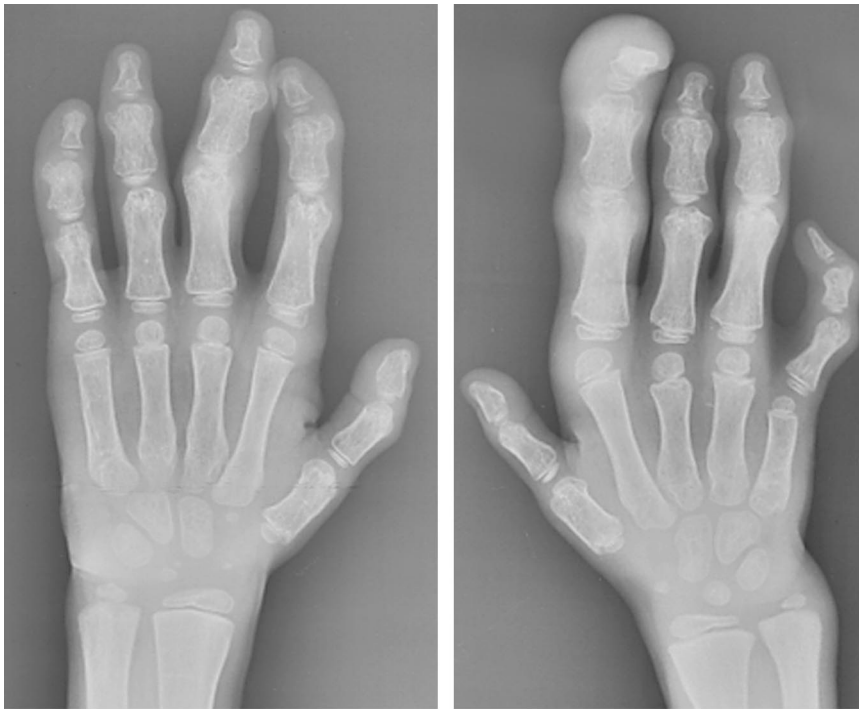
Manifestations of Proteus Syndrome

Progressive skeletal abnormalities such as macrodactyly, scoliosis, asymmetric overgrowth, and limb length discrepancy are the most frequent and striking findings in patients with Proteus syndrome, followed by soft-tissue abnormalities such as fatty, muscular, and vascular malformations. Visceral anomalies such as splenomegaly, asymmetric megalencephaly, white-matter abnormalities, and nephromegaly, as well as masses other than fatty, muscular, and vascular malformations, are less common.

Table 4
Radiologic Findings in Proteus Syndrome

Finding	Cases
Skeletal	
Macrodactyly	16
Clinodactyly	12
Asymmetric overgrowth or length discrepancy of limb	13
Abnormal vertebral bodies	13
Scoliosis	10
Hyperostosis	9
Bowing deformity	8
Focal calvarial thickening	6
Fused bones	6
Osteoporosis or osteopenia	6
Abnormal calcaneus	5
Asymmetric pelvic bones	5
Abnormal or discordant bone age	4
Coxa valga	4
Lytic lesions	4
Absent bones	3
Rib abnormalities	3
Hip subluxation or dislocation	2
Soft-tissue	
Abnormal or asymmetric fat distribution	13
Soft-tissue mass	9
Asymmetric muscle development	9
Connective tissue nevi of feet	9
Lipomas or focal fat overgrowth	7
Hypertrophic soft tissues	7
Vascular malformations	7
Soft-tissue calcifications	3
Muscular atrophy	2
Subcutaneous tissue thickening of feet	2
Visceral	
Splenomegaly	5
Nephromegaly	4
Hydrocele	4
Lung scarring	2
Emphysematous or cystic lung changes	2
Atelectasis	2
Central nervous system	
Asymmetric megalencephaly	4
White-matter abnormalities	4
Hydrocephalus	2
Cavernous venous malformation of brain	2
Lipomatosis of the spinal canal	2
Ear, nose, and throat	
Mastoid fluid or mucosal thickening	5
Paranasal sinus fluid or mucosal thickening	4
Abnormal middle ear	2

Note.—Each of the following was observed in one case: breast asymmetry, tracheal narrowing, enlarged portal vein, thyromegaly, thyroid nodule, hydronephrosis, renal calculi, gastromegaly, pancreatic lipomatosis, rectosigmoid polyposis, uterine leiomyomata, uterine (cervical) cysts, cystic lesion of right labium major, hypoplastic uterus, enlarged ovaries, varicocele, testicular microlithiasis, undescended testicle, epididymal cyst, arachnoid cyst, perineural cyst of right orbit, cystic changes of brain parenchyma, and schizencephaly.



a.

b.

Figure 2. Macrodactyly and clinodactyly. Posteroanterior radiographs of the left (a) and right (b) hands in a patient aged 2–3 years show asymmetric macrodactyly of the second through fifth left digits and of the second through fourth right digits; clinodactyly of the second, third, and fifth left digits and of the fifth right digit; osteoporosis of the right carpal, metacarpal, and phalangeal bones; and diffuse hypertrophy of the soft tissues in the second right ray.

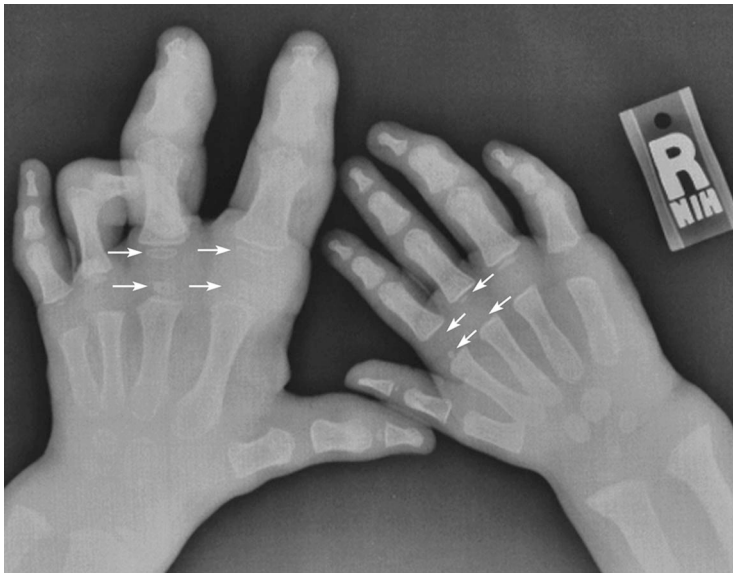


Figure 3. Asymmetric overgrowth and macrodactyly. Posteroanterior radiograph of the hands in a male patient aged 2–3 years shows asymmetric overgrowth of soft tissues and metacarpal and phalangeal bones in the left hand, particularly prominent in the second and third rays, and less prominent macrodactyly in the fourth and fifth rays in the right hand. Note the asymmetry of the ossification centers in the second and third rays (arrows).

Skeletal Abnormalities

Skeletal abnormalities are the most frequent finding in Proteus syndrome. Macrodactyly (Figs 2–4) is one of the most striking manifestations of Proteus syndrome. It may occur in association with clinodactyly (permanent medial or lateral deflection of one or more fingers). Syndactyly (fusion of the bones in fingers or toes, or webbing of the soft tissues between the digits) and polydactyly also are occasionally present. Macrodactyly was present in 16 (76%) of our 21 patients,

and clinodactyly (Figs 2, 3) was seen in 12 (57%). Asymmetric involvement of the hands (Fig 3) may cause abnormal or disharmonic bone age, which was seen in four (19%) of our 21 patients. Hyperostosis (Figs 5, 6) was seen in nine (43%) of the 21 patients. Asymmetric limb overgrowth and limb length discrepancy, which frequently occur in Proteus syndrome (Figs 3, 6–9), were found in 13 (62%) of our patients. The calcaneus

Figure 4. Rapid progression of macrodactyly and cerebriform connective-tissue nevus. **(a)** Anteroposterior radiograph of the right foot (same patient as in Fig 1), obtained at age 5 years, shows minimal overgrowth of bone. **(b)** Anteroposterior radiograph obtained 14 months later shows progressive overgrowth in the right foot; redundant lobulated plantar skin, characteristic of plantar cerebriform connective-tissue nevus (arrowheads); and macrodactyly of the right fifth toe, with a notched deformity in the midportion of the proximal phalanx (arrow).



a.

b.



5.

6.

Figures 5, 6. Hyperostosis. **(5)** Lateral radiograph of the right knee, obtained after deangulation osteotomy in a female patient aged 10 years, shows patellar and tibial hyperostosis (arrows), narrowing in the joint space, and irregular sclerosed surfaces in the patellofemoral and tibiofemoral compartments. **(6)** Anteroposterior radiograph of the knees in a patient aged 20 years shows asymmetric overgrowth of the soft tissues in the left lower extremity, as well as hyperostosis, deformity, and osteoporosis of the left distal femur and proximal tibia.



a. **b.**
Figure 7. Limb length discrepancy. Anteroposterior radiographs of the pelvis and thighs (**a**) and the legs and feet (**b**) of a 12-year-old male patient show asymmetric overgrowth of bones and soft tissues in the right side of the pelvis and the right lower extremity, limb length discrepancy, and bowing in the left femur and right fibula.

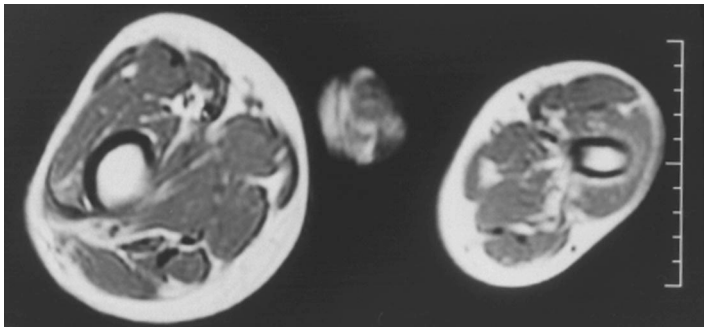
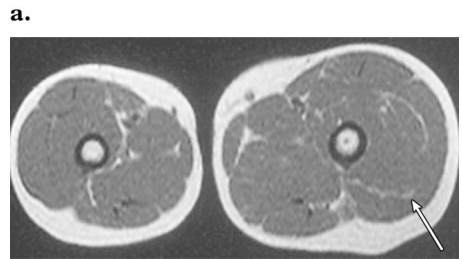
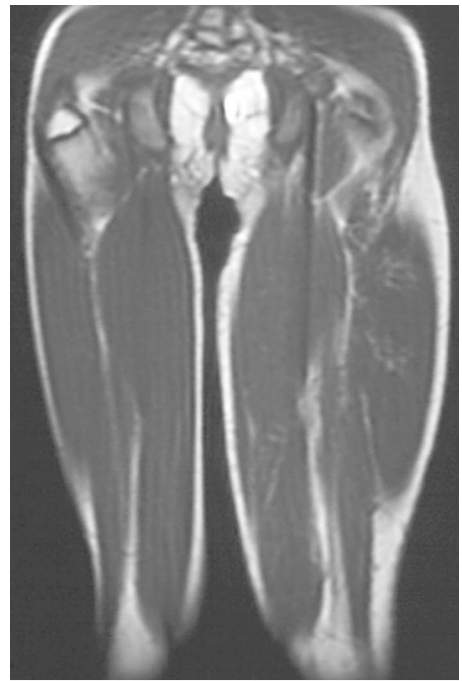
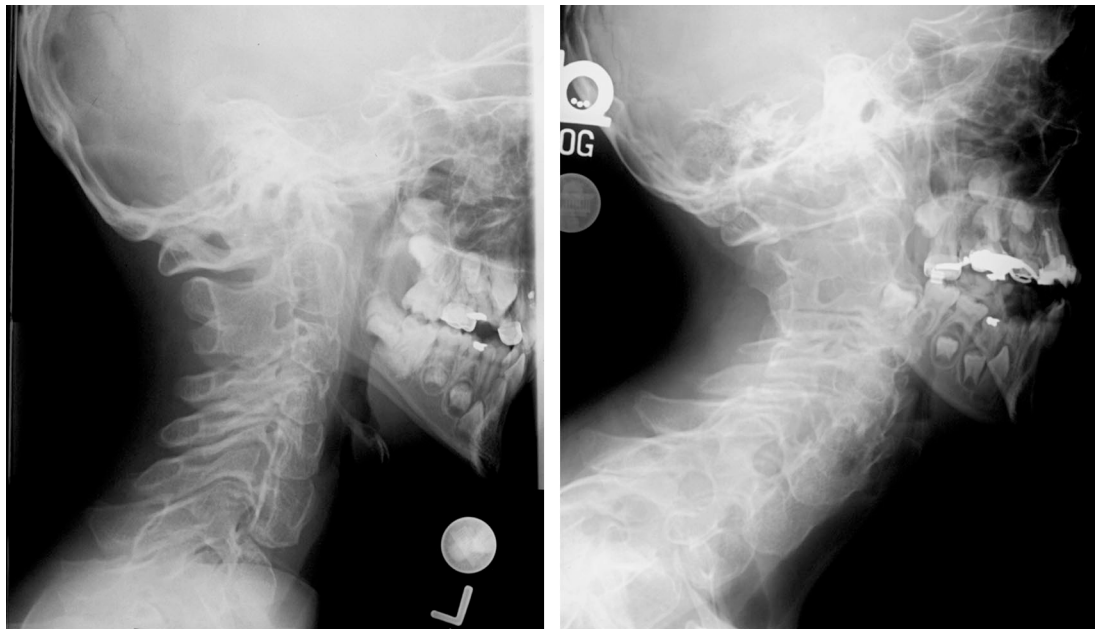
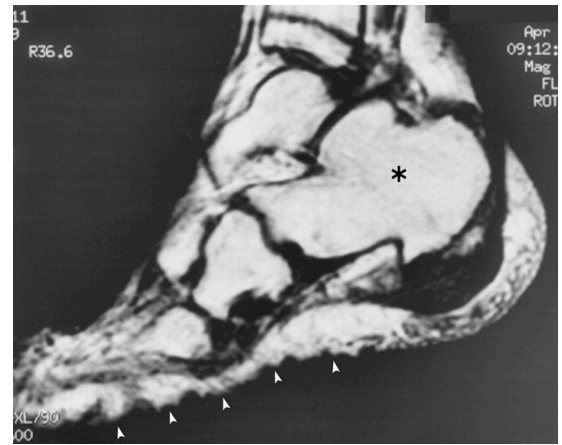


Figure 8. Asymmetric overgrowth. Axial T1-weighted MR image at the level of the upper thighs in a patient aged 7 years shows asymmetric overgrowth of the right femur and the muscles and subcutaneous tissues of the right thigh.



a.
b.
Figure 9. Asymmetric overgrowth. Coronal and axial T1-weighted MR images of the pelvis and thighs (**a**) and the middle thighs (**b**) in a patient aged 11 years show muscle and fat overgrowth in the left thigh and mild fatty infiltration (arrow in **b**) in the muscles of the left thigh.

Figure 10. Abnormal calcaneus and cerebri-form connective-tissue nevus. Sagittal T1-weighted MR image of the right foot in a patient aged 7 years shows disproportionate and dysmorphic enlargement of the calcaneus (*) and an irregular overgrowth of the plantar soft tissues that represents cerebri-form connective-tissue nevus (arrowheads).



a.

b.

Figure 11. Rapid progression of cervical spine overgrowth. **(a)** Right lateral radiograph obtained in a patient at age 6 years shows enlargement but relatively normal alignment of the cervical vertebral bodies. **(b)** Right lateral radiograph obtained at age 8½ years shows progressive enlargement of the vertebral bodies with resultant fixed hyperextension of the upper cervical spine and hyperflexion of the lower cervical spine, which led to a reduction in the patient's mobility.

was unusually large and distorted (Fig 10) in five (24%) of the 21 patients, in whom it caused gait disturbances. Spinal deformities also are a frequent finding in Proteus syndrome, and progressive spinal deformity is usually noted in childhood

(Fig 11). Abnormal vertebral bodies (Figs 12–14), observed in 13 (62%) of the 21 patients, are obvious and striking, and therefore they are a critical distinguishing feature of Proteus syndrome (Table 1). Asymmetric vertebrae were seen in four (19%) of the 21 patients, and scoliosis was present in 10 (48%). Craniofacial disfigurement caused by abnormal skull and facial

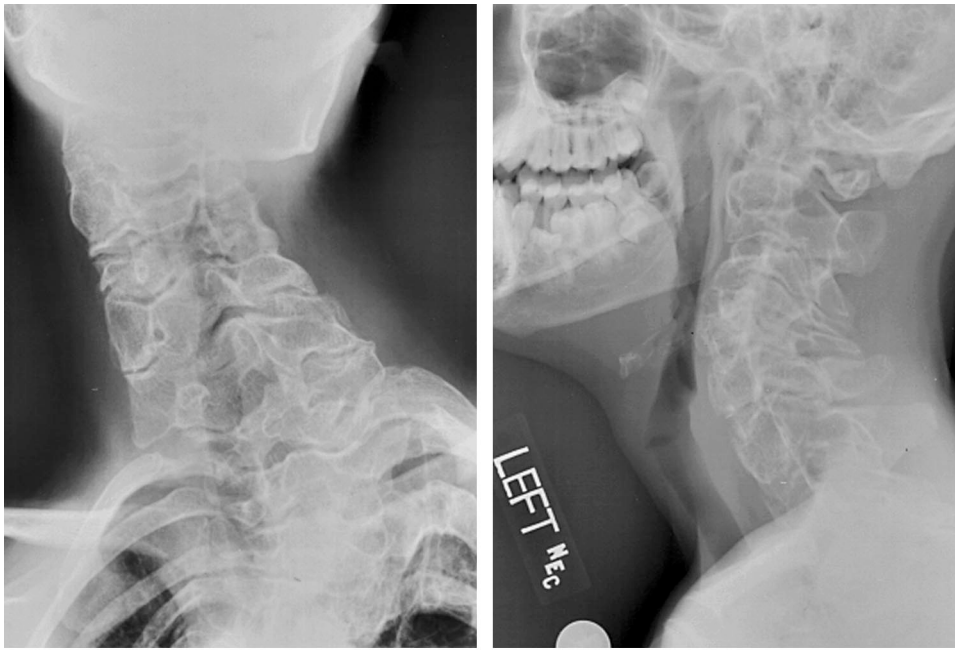
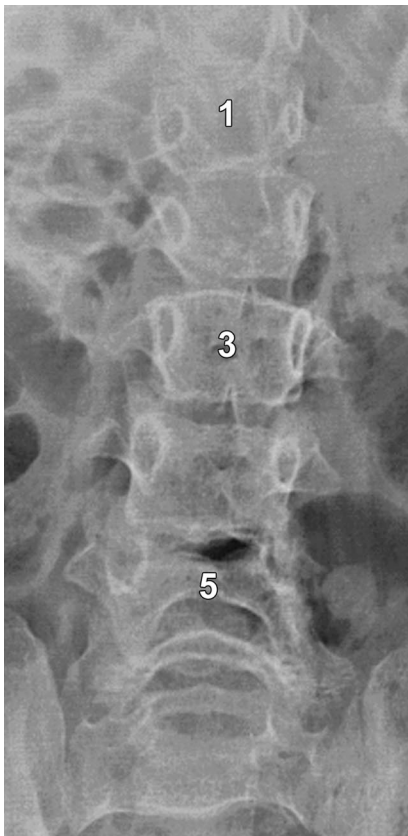


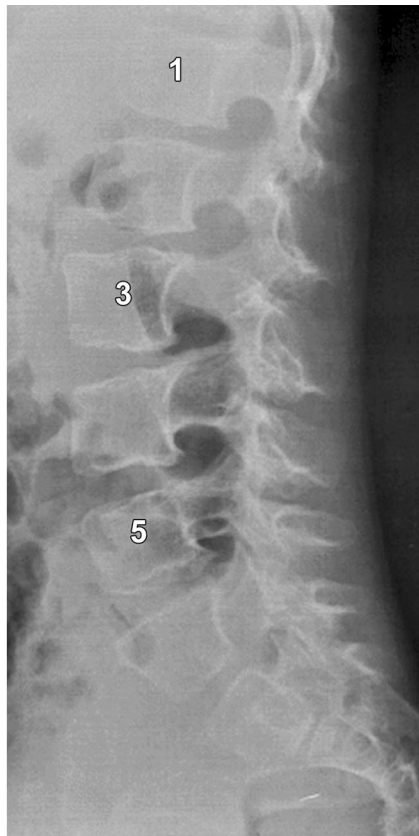
Figure 12. Abnormal vertebral bodies. Anteroposterior (a) and left lateral (b) radiographs of the cervical spine in a patient aged 16 years show asymmetric overgrowth of multiple vertebral bodies with resultant dextroscoliosis, hyperlordosis, and abnormal anteroposterior alignment of the upper cervical vertebral bodies, which led to a marked reduction in the patient's mobility. Note also the rib asymmetry and thoracic scoliosis in a.

a.

b.



13a.



13b.



14.

Figures 13, 14. Abnormal vertebral bodies. (13) Anteroposterior (a) and left lateral (b) radiographs of the lumbar spine in a patient aged 6 years show asymmetric overgrowth of multiple vertebral bodies and increased vertebral height, particularly of L3 and L4; lumbarization of S1; and posterior scalloping of all of the lumbar vertebral bodies, as well as S1. (14) Sagittal T1-weighted MR image of the thoracic spine in a patient aged 15 years shows marked variation in vertebral body shape and size, spondylosis at multiple levels, and posterior scalloping of several lower thoracic vertebrae, as well as thoracic kyphosis due to an abnormal midthoracic vertebral body (arrow).

Figure 15. Skull abnormalities. Sagittal (a) and axial (b) contrast-enhanced T1-weighted MR images of the head in a patient aged 5 years show several focal bone abnormalities, expansile lesions with abnormal accumulation of fatty tissue in several segments of the calvaria, and a focal defect in the outer table of the right occipital bone (arrowhead in b).

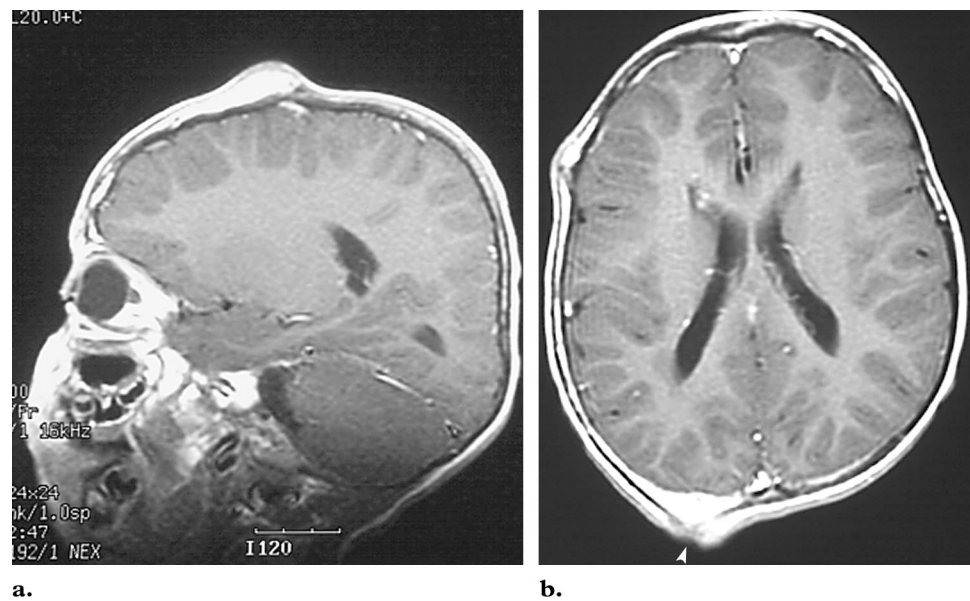


Figure 16. Skull abnormalities. (a) Axial CT image in a patient at age 3 months shows minimal calvarial thickening on the right side. (b) Axial MR image obtained with a fluid-attenuated inversion recovery, or FLAIR, sequence in the same patient at age 8 years shows expansile calvarial lesions with the signal intensity of fat in the frontal and right parietal bones (arrows); a lesion in the right parieto-occipital junction, probably a cavernous vascular malformation (arrowhead); and bilateral abnormalities in periventricular and deep white-matter signal intensities.

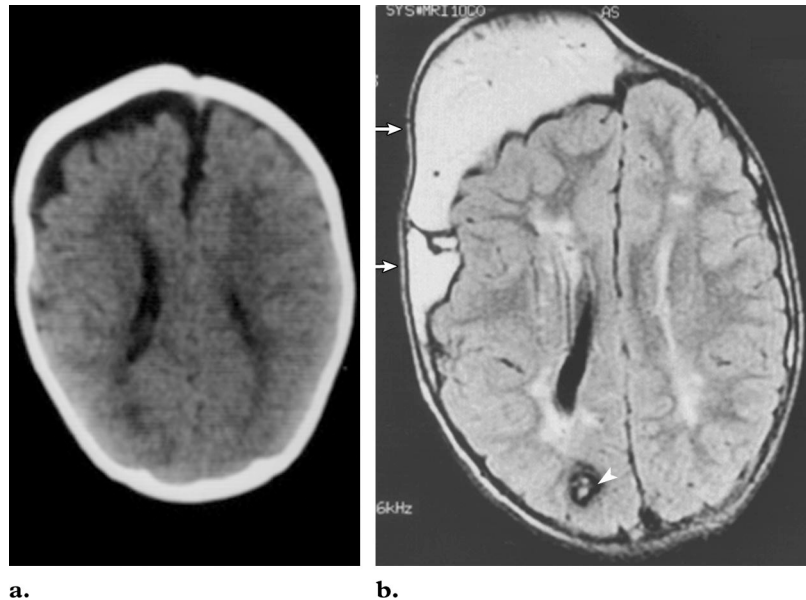


Figure 17. Severe pes equinus. Lateral radiograph of the right foot in a patient aged 17 years shows marked enlargement of the distal tibia and fibula; deformity and abnormal flexion of the calcaneus in the dorsal direction (black arrowhead); enlargement of the distal portion of the proximal phalanx, proximal portion of the distal phalanx, and the sesamoid bones of the first ray (arrows); coarse trabeculation of the enlarged bones; and lobulation of the plantar skin (white arrowheads), a finding that indicates cerebriform connective-tissue nevus.



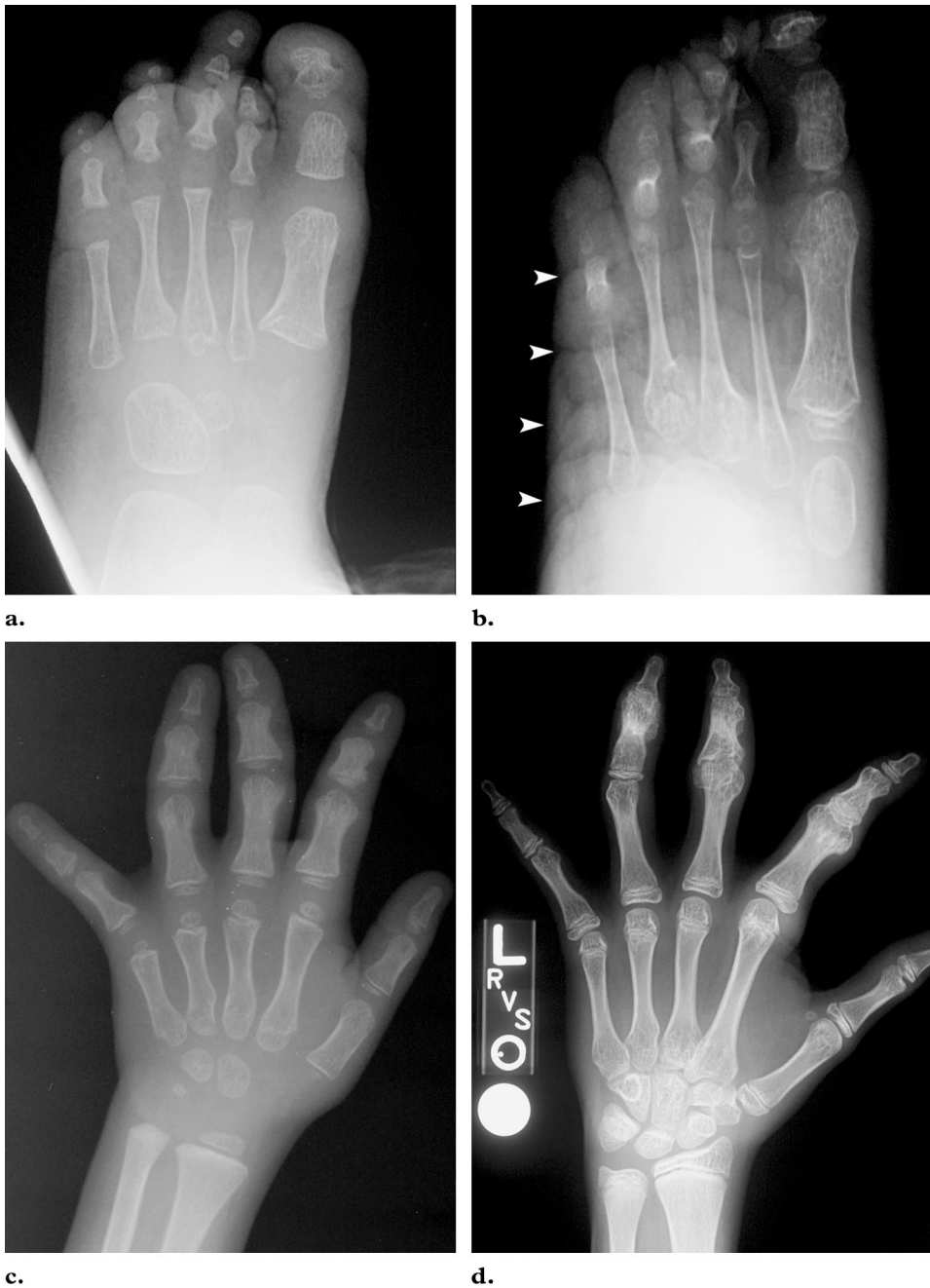


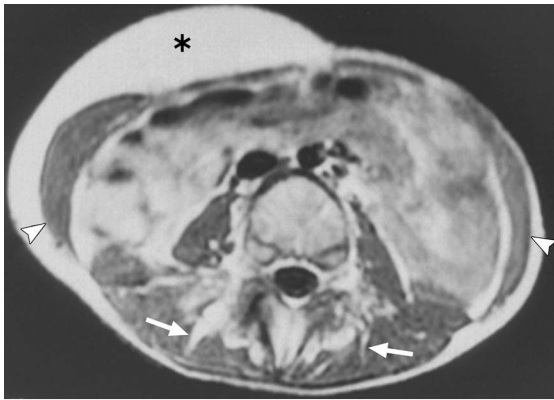
Figure 18. Progressive skeletal changes. (a, b) Anteroposterior radiographs of the left foot in a patient at ages 2 years (a) and 5 years (b) show progressive and disproportionate growth of the metatarsal and phalangeal bones of the toes, macrodactyly and clinodactyly, and a cerebriiform connective-tissue nevus (arrowheads in b). (c, d) Posteroanterior radiographs of the left hand in another patient at ages 4 years (c) and 16 years (d) show asymmetric and irregular overgrowth of the phalanges, more marked and with accompanying ankylosis of the interphalangeal joints in d.

growth is less common in Proteus syndrome than are skeletal abnormalities of the limbs and spine. Focal areas of severe calvarial thickening (Figs 15, 16) were found in the frontotemporal and parieto-occipital areas in six (29%) of our 21 patients. Deformities observed in the nasal bridge, alveolar dental ridges, and, rarely, external auditory canal were related to overgrowth of bone. In one of our patients, the calvarial lesions were very large and contained fatty tissue (Fig 16).

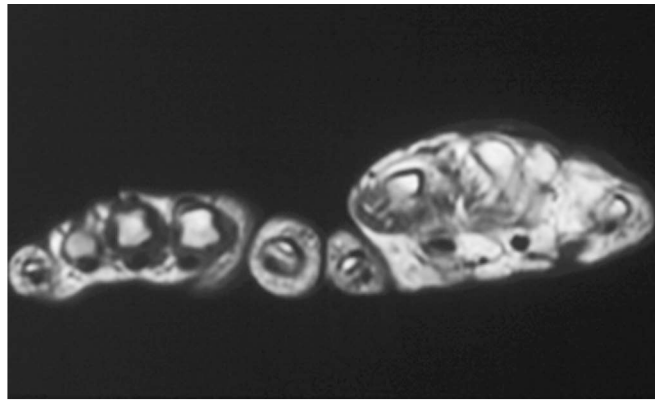
Some affected bones have a thin cortex and coarse trabeculation (Fig 17), and some appear demineralized (Figs 2, 6), findings that may be attributable to disuse. Specimens excised from the affected bones reportedly appear osteoporotic

and vascular but are histologically normal (13). However, the fact that there are few reports of fractures in patients with Proteus syndrome suggests that osseous strength overall is unaffected (13). One of the most characteristic findings in Proteus syndrome is the disorganization and distortion of skeletal features (Figs 6, 10, 17), a finding that contrasts strikingly with more common forms of osseous overgrowth in which the enlarged bones retain their normal proportional relationships. This finding, when accompanied by the typical rapid progression seen in Proteus syndrome (Figs 4, 11, 16, 18), is a key diagnostic criterion.

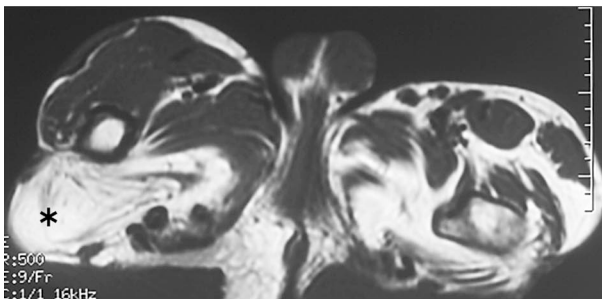
Figures 19–21. Fatty overgrowth. (19) Axial T1-weighted MR image through the level of the pelvis in a patient aged 8 years shows asymmetric adipose overgrowth along the anterior and lateral portion of the abdominal wall (*), asymmetry of the abdominal wall musculature (arrowheads), and fatty infiltration of the paraspinal muscles (arrows). (20) Axial T1-weighted MR image of the hands of a 28-year-old female patient shows marked asymmetry due to increased fatty components in the soft tissues of the right hand. The adipose overgrowth in this patient extended from the hand into the forearm. (21) Axial T1-weighted MR images of the pelvis and upper thighs (**a**) and the upper to middle thighs (**b**) in a patient aged 20 years show asymmetric muscle development in the thighs, asymmetric focal increase of fatty tissue in the right buttock (* in **a**), diffuse increase of fatty tissue in the left thigh, and focal accumulation of fat anterior to the left distal femur (arrow in **b**).



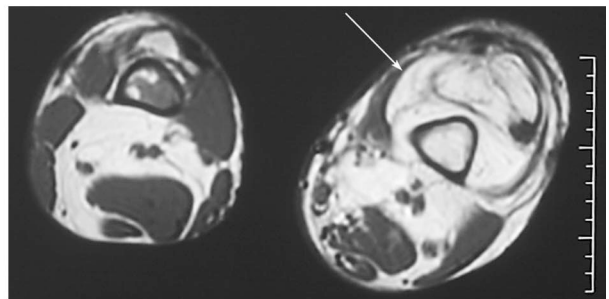
19.



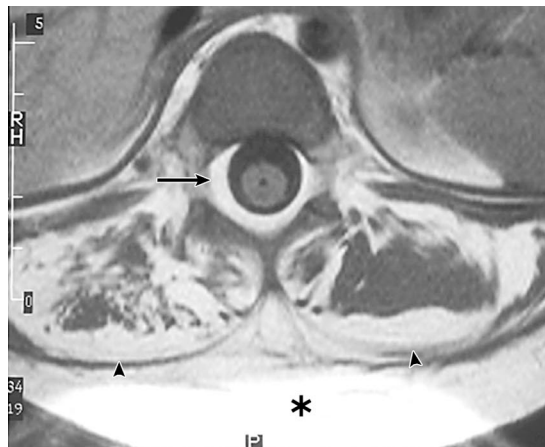
20.



21a.

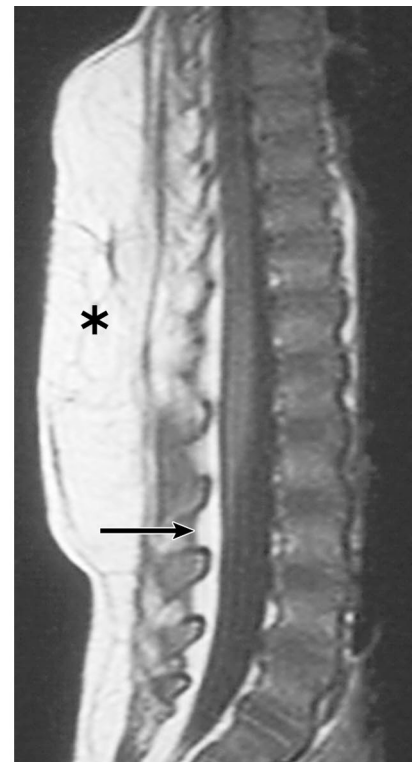


21b.



a.

Figure 22. Lipoma and fatty infiltration of muscles. Axial (**a**) and sagittal (**b**) T1-weighted MR images of the thoracic spine in a 6½-year-old female patient show a large lipomatous mass, posterior to the paraspinal muscle fascia, that extends from T6 to L5 (*), as well as asymmetric fatty infiltration and atrophy of the paraspinal muscles, right more than left (arrowheads in **a**), and increased fat in the spinal canal (arrow).

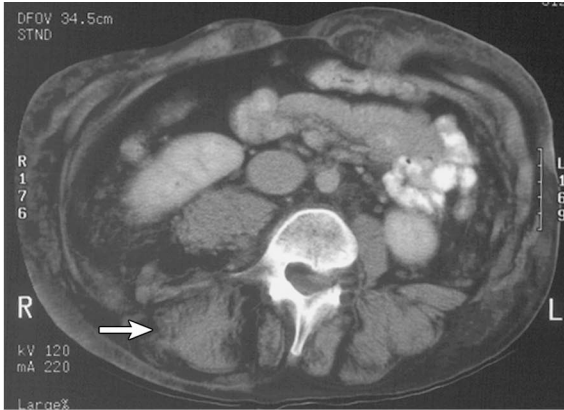


b.

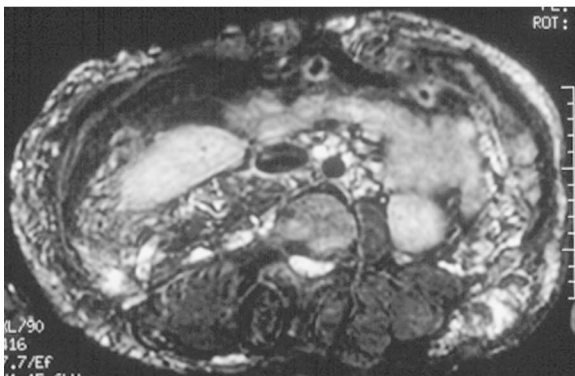
Figure 23. Fatty infiltration of muscles, and vascular malformations. **(a, b)** Axial nonenhanced CT images of the thorax **(a)** and abdomen **(b)** in a patient aged 14 years show thoracic deformity, including a large asymmetric area with the attenuation of fat along the posterior chest wall and infiltrating the paraspinal muscles bilaterally (arrows), more noticeable in the left side than in the right, which causes elevation of the left scapula away from the posterior chest wall (arrowhead in **a**); less prominent fatty infiltration along the left lateral chest wall and in the muscles of the anterior chest wall, as well as the posterior, lateral, and anterior abdominal wall and the left anterior rectus abdominis muscle; and enlargement of the right psoas muscle with fatty infiltration that surrounds multiple serpentine blood vessels. **(c)** Axial MR image obtained with a short inversion time inversion recovery, or STIR, sequence at a level similar to that in **b**, shows vascular malformations within the fatty tissue in the retroperitoneum, right psoas muscle, and abdominal wall.



a.



b.



c.

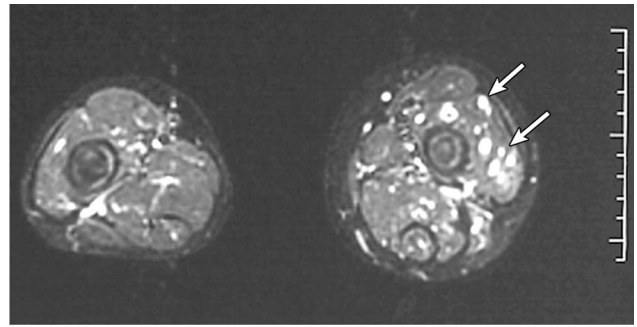
Soft-Tissue Abnormalities

Proteus syndrome is characterized by overgrowth of specific types of tissue. Adipose tissue overgrowth is most commonly manifested as asymmetry in the anterior or posterior body wall or in the subcutaneous fat of the extremities (Figs 19–

21). Overgrowth of fat and muscle may coexist and result in abnormally large muscle groups that contain interspersed fat (Figs 21–23). Adipose tissue overgrowth can be seen also in more

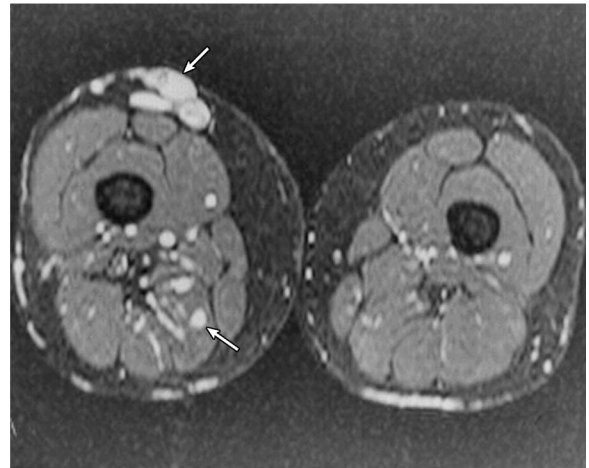


24a.



24b.

Figures 24, 25. (24) Fatty infiltration of muscles and vascular malformations. Axial MR images obtained with a short inversion time inversion recovery sequence in a patient aged 5 years at the levels of the pelvis (a) and thighs (b) show asymmetric fatty infiltration and numerous abnormal vascular structures in the muscles (arrows), more prominent on the left side than on the right. (25) Venous malformations. Axial MR image obtained with a short inversion time inversion recovery sequence at the level of the thighs in a patient aged 27 years shows multiple enlarged veins in the subcutaneous tissues and posterior muscles of the right thigh (arrows), as well as a slight enlargement of the right thigh with increased subcutaneous fat, which causes a mild asymmetry in the cross-sectional area of the thighs.



25.

complex soft-tissue enlargements that contain lymphatic, capillary, or venous vascular malformations combined with fat (Figs 23–25). Diffuse and infiltrating vascular malformations (lymphatic, venous, or capillary) were present in seven (33%) of our 21 patients.

Diffuse, abnormal, or asymmetric distribution of adipose tissue was seen in 13 (62%) of the 21 patients. Asymmetric muscle development was seen in nine (43%) of the 21 patients. Muscular calcifications are infrequent in Proteus syndrome, but their presence should bring this entity into the differential diagnosis. We saw muscular calcifications in three (14%) of our 21 patients. Connective-tissue nevi that cause a corrugated appearance of the skin, particularly in the plantar aspect

of the foot (Figs 1, 4, 10, 17, 18), are a highly specific finding but are not universal among patients with Proteus syndrome. Commonly referred to as moccasin sole or cerebriform nevus, such findings were seen in nine (43%) of our patients. These changes were readily detected both with MR imaging and with CT and were obvious at clinical evaluation. MR imaging was useful also for identifying abnormalities in the underlying bones of the foot (Fig 10).

Visceral Abnormalities

Visceral anomalies in Proteus syndrome are less common than musculoskeletal and soft-tissue abnormalities. The visceral anomalies most frequently seen in our patients (Figs 26, 27) were

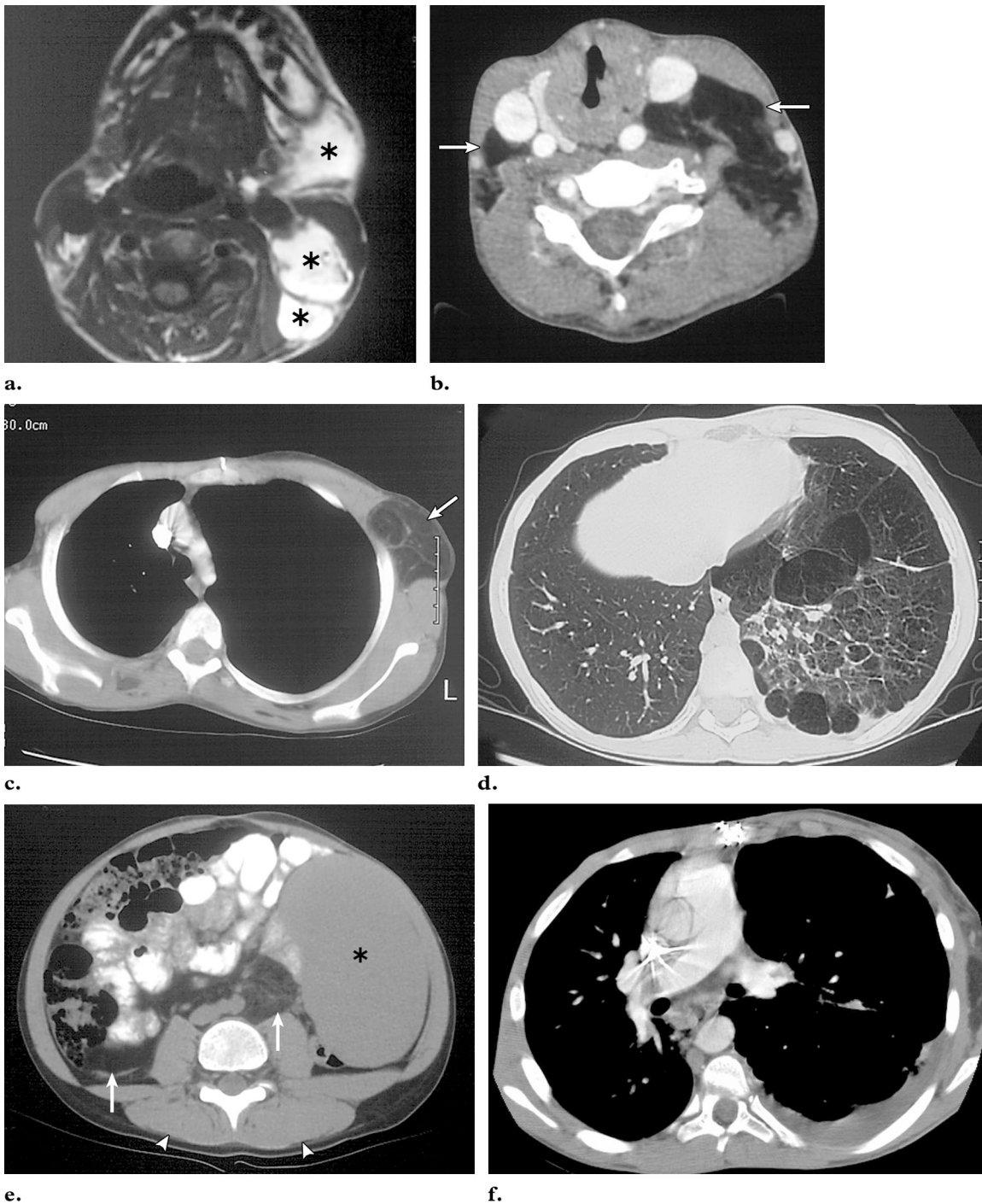


Figure 26. Lipomas, splenomegaly, cystic lung changes, and pulmonary embolism. **(a)** Axial T1-weighted MR image obtained in a patient aged 11 years at the level of the mandible shows asymmetric fatty masses (*) anterior to, and under, the sternocleidomastoid muscles, a finding more prominent in the left side than the right. **(b)** Axial CT image obtained at a level below **a**, in the neck, shows multiple bilateral asymmetric masses with the attenuation of fat (arrows), more prominent in the left side than the right, and causing deviation of the midline structures in the neck to the right. **(c)** Axial CT image at the level of the upper thorax shows asymmetric overgrowth of fat in the anterior thoracic wall, a focal fatty lesion in the left axilla (arrow), deviation of the mediastinum to the right, and asymmetry of the thorax, with the left hemithorax larger than the right. **(d)** Axial CT image at the level of the lower thorax depicts hyperexpansion of the left lung and areas of severe scarring and cystic changes in the left lower lobe, as well as mild cystic changes in the right lower lobe. **(e)** Axial CT image of the abdomen shows increased retroperitoneal fat (arrows); asymmetric development of the paraspinal muscles (arrowheads), with the left side greater than the right; and marked splenomegaly (*). **(f)** Contrast-enhanced CT image of the chest obtained 4 years later shows filling defects in the lower lobes of the right and left lungs because of emboli in the pulmonary arteries, as well as a small left pleural effusion.

splenomegaly, seen in five (29%) of 17 patients with visceral anomalies; and asymmetric megalencephaly, white-matter abnormalities, and nephromegaly, each of which was seen in four (24%) of these 17 patients. Cystic lung changes and pulmonary emboli (Fig 26) also have been reported to occur in association with Proteus syndrome (5,7–9). Cystic and emphysematous lung changes were detected in two of our 21 patients, and pulmonary embolism was the cause of death in two patients. Acute pulmonary embolism was diagnosed also in two other patients in this cohort during the study period: One of the two, a 16-year-old male patient, experienced two episodes of pulmonary embolism while recovering from endoscopy for gastrointestinal hemorrhage. In the second patient, a 32-year-old woman, acute pulmonary embolism was diagnosed during convalescence after a tibial osteotomy. Anticoagulant therapy was begun immediately after diagnosis of embolism, and both patients recovered.

Tumors

Neoplasms associated with Proteus syndrome include lipomas, ovarian cystadenomas, and monomorphic parotid adenomas (1). Lipomas, like nearly all tissue overgrowths in Proteus syndrome, are not truly neoplastic but instead are secondary to hyperplasia. Unlike lipomas that occur in other disorders, lipomas in Proteus syndrome tend to grow aggressively and may infiltrate the muscles or invade the spinal canal (1,14–17). We saw lipomas or focal fat overgrowth (Figs 19–23, 26) in seven of our patients, adipose tissue infiltration of muscle in five patients, and adipose tissue invasion of the spinal canal (Figs 22, 23) in two patients. None of our patients, however, had symptoms of spinal compromise. In this respect, our findings did not bear out previously published reports of patients with Proteus syndrome and spinal compression from invasive lipomas (15,17). It is not possible, on the basis of our data, to distinguish lesions that will cause spinal compromise from those that will not. It is difficult to recommend surgery for these lesions unless symptoms are present, but it is equally difficult to resect such lesions after spinal

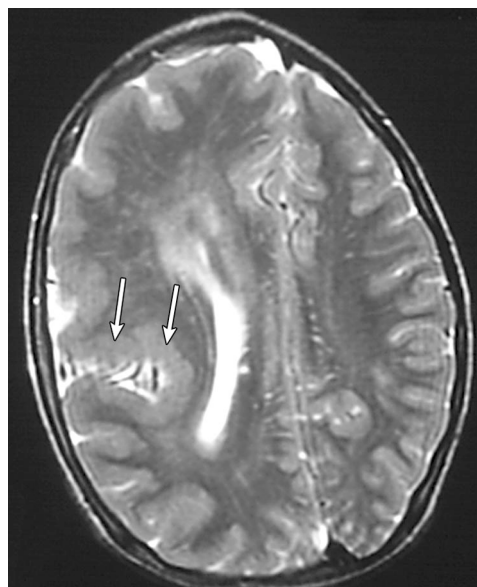


Figure 27. Asymmetric megalencephaly. Axial T2-weighted MR image of the head of a patient aged 7 years shows broad gyration and diffuse enlargement of the right cerebral hemisphere, closed-lip schizencephaly beginning at the right lateral sulcus (arrows), and prominence of the Virchow-Robin spaces.

involvement has occurred. Appropriate techniques for managing these lesions cannot be devised without additional data.

Less common neoplasms associated with Proteus syndrome include benign tumors such as meningioma, ovarian cystadenoma, and monomorphic adenoma of the parotid gland, and, even rarer, malignant neoplasms such as papillary adenocarcinoma of the testis, mesothelioma of the tunica vaginalis, and peritoneal mesothelioma (1,14). Although we did not see any of these uncommon tumors in our study population, the radiologist should keep in mind their possible occurrence in association with Proteus syndrome.

Differential Diagnosis

Because the manifestations of Proteus syndrome are highly variable and many are found also in other overgrowth syndromes, diagnosis can be difficult. In the absence of a specific genetic test, the diagnosis of Proteus syndrome depends on clinical and radiologic findings. Therefore, the radiologist plays an important role in evaluation, diagnosis, and management of the condition. Several articles about the differential diagnosis of

Proteus syndrome have been published (6,12). Disorders included in the differential diagnosis of Proteus syndrome are listed in Table 3. The disorders most commonly confused with Proteus syndrome are Klippel-Trénaunay syndrome, neurofibromatosis type 1, and hemihyperplasia-multiple lipomatosis syndrome (6,12). Other overgrowth disorders, such as Maffucci syndrome and Bannayan-Riley-Ruvalcaba syndrome, are sometimes confused with Proteus syndrome. Klippel-Trénaunay syndrome is an uncommon disorder characterized by a triad of clinical findings that may include unilateral cutaneous capillary or venous vascular malformations, as well as overgrowth of the underlying bone and soft tissue, typically in a lower extremity (18). The tissue overgrowth in Klippel-Trénaunay syndrome is usually associated with vascular malformations, whereas in Proteus syndrome the overgrowth of bone and other tissues may occur independently of vascular malformations. Klippel-Trénaunay syndrome less frequently occurs bilaterally, and, on rare occasions, may affect an upper extremity. Multiple calcified phleboliths within pelvic venous malformations can be seen on radiographs of the abdomen (19). In Proteus syndrome, limb overgrowth is usually absent or mild at birth, whereas in Klippel-Trénaunay syndrome it is present at birth and is commonly severe (6). Progressive irregular and dysplastic overgrowth of bone, which is typical of Proteus syndrome (Figs 4, 11, 16, 18), is not seen in Klippel-Trénaunay syndrome and therefore is a key radiologic distinction. In Parkes Weber syndrome (a variant of Klippel-Trénaunay syndrome), limb hypertrophy is associated with arteriovenous malformations (19).

Neurofibromatosis type 1, a disease caused by mutations in the *NF1* gene on chromosome 17 (20), is inherited in an autosomal dominant pattern and is characterized by Lisch nodules, axillary freckles, multiple café-au-lait spots, and multiple neurofibromas. These signs are absent in Proteus syndrome (12,20).

Maffucci syndrome is a rare disorder characterized by multiple enchondromas and multiple capillary and venous malformations. The presence of venous malformations with phleboliths in the soft tissues differentiates Maffucci syndrome from Ollier disease (21). Enchondromas have not been reported in Proteus syndrome.

Bannayan-Riley-Ruvalcaba syndrome is also inherited in an autosomal dominant pattern and

is associated with mutations in the *PTEN* gene on chromosome 10q. It is characterized by generalized polyposis of the colon and rectum, macrocephaly, pigmented macules of the penis, lipomas, capillary vascular malformations, and Hashimoto thyroiditis (22,23). The specific genetic characteristics of Bannayan-Riley-Ruvalcaba syndrome and its distinct phenotype set it apart from Proteus syndrome. Some other patients with *PTEN* mutations have atypical (non-Bannayan-Riley-Ruvalcaba syndrome) overgrowth phenotypes. These patients do not meet the diagnostic criteria for Proteus syndrome, in spite of claims to the contrary (24,25).

Conclusions

Proteus syndrome is characterized by progressive mosaic overgrowth of skin, bones, muscles, fatty tissues, and blood and lymphatic vessels, as well as by visceromegaly, lung cysts, and predisposition to pulmonary embolism. The syndrome is rarely associated with benign or malignant tumors. The variable nature of the signs of Proteus syndrome makes its diagnosis challenging. Until a specific genetic test is available, diagnosis and management will depend entirely on the results of physical examination and imaging studies. Knowledge of the multiple highly specific radiologic manifestations of Proteus syndrome is therefore essential for diagnosis of this condition. The appropriate use of imaging modalities and published diagnostic criteria will greatly increase the accuracy of diagnosis.

Acknowledgments: The authors thank the families that participated in this study, the numerous radiologists who contributed outside images or interpreted images at the NIH Clinical Center, and M. M. Cohen, Jr, for reviewing a previous draft of the manuscript. The study would not have been possible without the support of Proteus syndrome foundations in the United States and the United Kingdom (www.proteus-syndrome.org and www.proteus-syndrome.org.uk, respectively).

References

1. Cohen MM Jr. Proteus syndrome: clinical evidence for somatic mosaicism and selective review. *Am J Med Genet* 1993; 47:645-652.
2. Levine C. The imaging of body asymmetry and hemihypertrophy. *Crit Rev Diagn Imaging* 1990; 31:1-80.

3. Hamm H. Cutaneous mosaicism of lethal mutations. *Am J Med Genet* 1999; 85:342-345.
4. Cohen MM Jr, Hayden PW. A newly recognized hamartomatous syndrome. *Birth Defects Orig Artic Ser* 1979; 15:291-296.
5. Wiedemann HR, Burgio GR, Aldenhoff P, Kunze J, Kaufmann HJ, Schirg E. The proteus syndrome: partial gigantism of the hands and/or feet, nevi, hemihypertrophy, subcutaneous tumors, macrocephaly or other skull anomalies and possible accelerated growth and visceral affections. *Eur J Pediatr* 1983; 140:5-12.
6. Biesecker LG, Happle R, Mulliken JB, et al. Proteus syndrome: diagnostic criteria, differential diagnosis, and patient evaluation. *Am J Med Genet* 1999; 84:389-395.
7. Eberhard DA. Two-year-old boy with Proteus syndrome and fatal pulmonary thromboembolism. *Pediatr Pathol* 1994; 14:771-779.
8. Slavotinek AM, Vacha SJ, Peters KF, Biesecker LG. Sudden death caused by pulmonary thromboembolism in Proteus syndrome. *Clin Genet* 2000; 58:386-389.
9. Cohen MM Jr. Causes of premature death in Proteus syndrome. *Am J Med Genet* 2001; 101:1-3.
10. Treves F. *The elephant man and other reminiscences*. London, England: Cassell, 1923.
11. Happle R. Lethal genes surviving by mosaicism: a possible explanation for sporadic birth defects involving the skin. *J Am Acad Dermatol* 1987; 16:899-906.
12. Samlaska CP, Levin SW, James WD, Benson PM, Walker JC, Perlik PC. Proteus syndrome. *Arch Dermatol* 1989; 125:1109-1114.
13. Stricker S. Musculoskeletal manifestations of Proteus syndrome: report of two cases with literature review. *J Pediatr Orthop* 1992; 12:667-674.
14. Gordon PL, Wilroy RS, Lasater OE, Cohen MM Jr. Neoplasms in Proteus syndrome. *Am J Med Genet* 1995; 57:74-78.
15. Ring D, Snyder B. Spinal canal compromise in Proteus syndrome: case report and review of the literature. *Am J Orthop* 1997; 26:275-278.
16. Whitley JM, Flannery AM. Lymphangiolioma of the thoracic spine in a pediatric patient with Proteus syndrome. *Childs Nerv Syst* 1996; 12:224-227.
17. Skovby F, Graham JM Jr, Sonne-Holm S, Cohen MM Jr. Compromise of the spinal canal in Proteus syndrome. *Am J Med Genet* 1993; 47:656-659.
18. Cohen MM, Neri G, Weksberg R. Overgrowth syndromes. In: *Oxford monographs on medical genetics*. No. 43. Oxford, England: Oxford University Press, 2002.
19. Goldman AB. Heritable diseases of connective tissue, epiphyseal dysplasias, and related conditions. In: Resnick D, ed. *Diagnosis of bone and joint disorders*. Philadelphia, Pa: Saunders, 1996.
20. Lane B, Stevens JM, Moseley IF. Cranial and intracranial pathology: malformations, trauma, bone pathology, CSF disturbances. In: Grainger RD, Allison DJ, eds. *Grainger & Allison's diagnostic radiology: a textbook of medical imaging*. New York, NY: Churchill Livingstone, 1997.
21. Stoker DJ. Bone tumours: general characteristics, benign lesions. In: Grainger RD, Allison DJ, eds. *Grainger & Allison's diagnostic radiology: a textbook of medical imaging*. New York, NY: Churchill Livingstone, 1997.
22. Gorlin RJ, Cohen MM Jr, Condon LM, Burke BA. Bannayan-Riley-Ruvalcaba syndrome. *Am J Med Genet* 1992; 44:307-314.
23. Longy M, Coulon V, Duboue B, et al. Mutations of PTEN in patients with Bannayan-Riley-Ruvalcaba phenotype. *J Med Genet* 1998; 35:886-889.
24. Zhou XP, Marsh DJ, Hampel H, Mulliken JB, Gimm O, Eng C. Germline and germline mosaic PTEN mutations associated with a Proteus-like syndrome of hemihypertrophy, lower limb asymmetry, arteriovenous malformations and lipomatosis. *Hum Mol Genet* 2000; 9:765-768.
25. Smith JM, Kirk EP, Theodosopoulos G, et al. Germline mutation of the tumour suppressor PTEN in Proteus syndrome. *J Med Genet* 2002; 39:937-940.